

Responses to recommendations

Comments

Due to the emission uncertainties in air quality modeling prediction, the development of air quality diagnostic prediction method could be practical based on the understanding of the physical connection of meteorological parameters to air quality change. Therefore, the establishment and application of PLAM/h Index (Parameter Linking Air-quality to Meteorological conditions/haze) in this paper are of considerable interest. For the benefit of the reader, however, a number of points need clarifying and certain statements require further justification.

Major comments:

1) With modifying the initial meteorological PLAM (Wang et. al., 2012) with the 2010 PM2.5 emission data, a new parameter PLAM/h is developed for haze forecast. Please note that a) these PM2.5 emission data provide only the primary emission, and the secondary aerosol particles contribute more than half PM2.5 to haze formation in China. This contribution of secondary aerosols with their precursor emission should be considered into the PLAM/h development;

Response: We agree with the reviewer's good advice that the contribution of secondary aerosols with their precursor emissions should be considered into the PLAM/h development. For the current development of PLAM/h, the primary emissions are used as an indicator for the emission spatial distributions and NOT a quantitative input for the model.

We will do the further optimizations for the secondary aerosol potential contributions to fully engage emission inventories in PLAM/h.

2) To quantify the impact of emission in PLAM index, the probability of its impact on the surrounding area are isotropic in the section 2.3, which is discussible, because the pollutant emissions could influence on the downstream area driven by winds (not all the surrounding areas).

Response: Thanks for your advice. The "isotropic" is as a first order approximation to emissions. Impact from downstream wind is expressed by the meteorological conditions.

3) Based on the Figure 2, the two regression lines of PLAM and PLAM/h (see the following Fig.) present less differences in visibility prediction, especially for haze weather (Vis. <10km).

Response: Figure 2 shows that a reasonable correlation exists between PLAM/h and visibility regardless of emission contributions and the difference between red and black-dashed lines is not visually obvious. However, the determination coefficient (R^2) is increased from 0.3675 to 0.3887 when emissions are considered, indicating the importance of inclusion of emission in PLAM/h. (lines 223-224 in the revised manuscript)

4) This paper uses the near real-time (NRT) operational data, including surface observation data. Please clarify the NRT data, which are the modeling forecast data or observation data. How can these data be used to 24h forecast?

Response: As a parameterization method, PLAM/h uses the NRT observation data for a short time or short term forecast. The NRT atmospheric observation data are used in the Equations (4,5 and 6) to calculate q_s (humidity), f_c (condensation function), and (wet-equivalent potential temperature) etc, which then are substituted into the Equation (3) to obtain the "static stability" of air masses in the diagnosis and trend prediction of air quality.

5) The English language should be substantially improved. For example, please use "haze" to replace and correct "atmospheric fog-haze", "fog-haze" "visibility fog-haze", all of which are Chinese English "haze".

Response: Thank you for suggestions. Further changes were made for the modification of the English language.

Specific comments:

1) In this paper, the coefficient of determination R^2 is used in analyzing correlation between visibility and PLAM Index. It cannot be called the correlation coefficient. The correlation coefficient is R . (line 24,223,315,371,387,423...)

Response: Thank you for suggestions. Modifications are made, in R^2 . (marked with edit-note in position (lines 23,223,316,372,388,413,435,565) of the revised manuscript)

2) The correlation fitted lines of PLAM index value without emission are marked by yellow dashed line instead of "black dashed line" . (line 220)

Response: Modified figure 2: The correlation fitted lines of PLAM index value without emission are marked by yellow dashed line instead of “black dashed line” . (line 221 of the revised manuscript)

3) According to Fig. 4a, when $PLAM < 100$, visibility is not less than 10 km, but larger than 10 km. (line 323)

Response: Modify text associated as follow: replace “ <100 ” to “ <150 ” , replace “ <10 km” to “ >10 km” (line 323 of the revised manuscript)

4) In Fig. 5, R_2 is always less than 1, so the value of the figure should be between 0-1, but not between 0-100.

Response: Figure 5 modified: “the icon for 0-100%, drawing the R_2 value magnified 100 times in Fig.5” (lines 344-345 of the revised manuscript)

Remarks from the typesetter in ACPD file

TS1 Please provide timezone throughout text.

TS2 Please provide page range or DOI.

TS3 Please provide page range or DOI.

TS4 Please provide volume number and page range or article number.

TS5 Please provide page range or DOI.

TS6 Please provide title.

TS7 Please provide article title.

TS8 Please provide volume number and page range or article number.

TS9 Please provide page range or article number + DOI.

Response: Provided (UTC+8) for timezone (TS1) throughout the revised manuscript.

Reference has been modified corresponding to TS2-TS9 (lines 470,473,489,490,493,500 and 516 respectively in the revised manuscript) .

1 **PLAM – A Meteorological Pollution Index for Air Quality and its**
2 **Applications in Fog-Haze Forecasts in North China**

3 **Yuanqin Yang¹, Jizhi Wang^{1*}, Sunling Gong^{1*}, Xiaoye Zhang¹, Hong Wang¹,**
4 **Yaqing Wang¹, Jie Wang², Duo Li³ and Jianping Guo¹**

5
6 1 Institute of Atmospheric Composition/Key Laboratory of Atmospheric Chemistry of
7 China Meteorological Administration (CMA), Chinese Academy of Meteorological
8 Sciences (CAMS), Beijing 100081, China

9 2 National Meteorological Information Centre, CMA, Beijing 100081, China

10 3 National Climate Centre, CMA, Beijing 100081, China

11
12 * Corresponding author: Sunling@cams.cma.gov.cn; wjz@cams.cma.gov.cn

13
14 **Abstract:** Using surface meteorological observation and high resolution emission data,
15 this paper discusses the application of PLAM/h Index (Parameter Linking Air-quality
16 to Meteorological conditions/haze) in the prediction of large-scale low visibility and
17 fog-haze events. Based on the two-dimensional probability density function diagnosis
18 model for emissions, the study extends the diagnosis and prediction of the
19 meteorological pollution index PLAM to the regional visibility fog-haze intensity. The
20 results show that combining the influence of regular meteorological conditions and
21 emission factors together in the PLAM/h parameterization scheme is very effective in
22 improving the diagnostic identification ability of the fog-haze weather in North China.

23 The **determination** coefficients for four seasons (spring, summer, autumn and winter)
24 between PLAM/h and visibility observation are 0.76, 0.80, 0.96 and 0.86 respectively
25 and all their significance levels exceed 0.001, showing the ability of PLAM/h to predict
26 the seasonal changes and differences of fog-haze weather in the North China region.
27 The high-value correlation zones are respectively located in Jing-Jin-Ji (Beijing,
28 Tianjin, Hebei), Bohai Bay rim and the southern Hebei-northern Henan, indicating that
29 the PLAM/h index has relations with the distribution of frequent heavy fog-haze
30 weather in North China and the distribution of emission high-value zone.
31 Comparatively analyzing the heavy fog-haze events and large-scale fine weather
32 processes in winter and summer, it is found that PLAM/h index 24 h forecast is highly
33 correlated to the visibility observation. Therefore, PLAM/h index has better capability

带格式的: 字体: (默认) Times
New Roman, 小四, 突出显示

删除的内容: correlation

35 of doing identification, analysis and forecasting.

36

37 **Key Words:** meteorological condition, PLAM index method, fog-haze in North China,
38 diagnostic prediction

39

40 **1 Introduction**

41 Compared with 1980s, fog-haze pollution events have increased significantly in
42 the recent decade in the Beijing and North China region. Meteorological condition is
43 one of the important elements that impact the local aerosol accumulation and
44 contributes to the frequent appearance of low visibility weather (Wang et al., 2010,
45 Wang, et al., 2002). The synthetic impact analysis on the pollution-related atmospheric
46 dynamic, thermodynamic and chemical processes as well as the fog-haze prediction
47 study has drawn widely attentions. Long-term observations have pointed out that in the
48 last 30 years fog-haze phenomenon in the central and eastern part of China has become
49 more and more serious due to anthropogenic emissions. Under some meteorological
50 conditions, aerosol particles in the atmosphere can be activated into cloud condensation
51 nuclei (CCN), participating in the formation of clouds and fog, which means that
52 modern fog-haze have involved lots of polluted aerosol particles (e.g. PM_{2.5}). To
53 reduce the impact of the weather disaster of fog-haze, special attentions need to be
54 given to atmospheric aerosol pollution (Zhang, et al., 2013) The 3-dimensional
55 numerical model has been progressed in different degrees in the meteorological
56 services of the global air quality predictions(McKeen, 2007; Moran, 2009;
57 Zhang, 2009). Chemical forecasting model study and prediction usually faces the
58 problems of timely emission data all over the world, therefore limits the ability to
59 improve the forecasting accuracy. In recent years, through analyzing the observation
60 data of atmospheric aerosol particulate matter (PM) and the physical connection of
61 sensitive meteorological parameters, the establishment of air quality parameterized
62 diagnostic predicting method has being developed. Research results revealed that the
63 air quality meteorological index PLAM (Parameter linking Air-quality to
64 Meteorological conditions) can achieve reasonable results when it was applied in the
65 prediction of the air quality in Beijing during the 2008 Beijing Olympic Games. The
66 identification and prediction researches of meteorological condition PLAM index to air
67 quality have achieved progresses at home and abroad in recent years (Zhang et al.,

68 2009; Honoré et al., 2008; Li et al.; 2010; Kassomenos, et al., 2008; Yang, et al., 2009 ;
69 Wang et al., 2013). Researches indicate that the contribution of meteorological
70 condition PLAM index from emissions is of great importance as they have remarkable
71 impacts on the regional distribution of air qualities in different areas. However, there
72 are very limited researches on emission contribution to the air quality meteorological
73 index, including its quantitative expression, physical mechanism and diagnostic
74 prediction. This is especially critical in establishing the relations and mechanism of
75 large-scale high-value $PM_{2.5}$ and low visibility weather.

76 On the basis of parameterized meteorological condition principle method, this
77 paper is to discuss the mutual impact of emission and meteorological condition, and
78 study the structure and function of meteorological conditions PLAM index in
79 quantitatively identifying, diagnosing and forecasting large scope of fog-haze weather.

80

81 **2 Data and methods**

82 This paper uses the near real-time (NRT) operational data, including surface
83 observation data, from which the elements related to meteorological condition impact
84 are extracted such as atmospheric temperature, difference of temperature and dew point,
85 clouds, weather phenomenon, air pressure, wind direction and speed and visibility, and
86 high-level sounding data as well as the data from atmospheric component observing
87 system stations. The multi-source element data including high resolution emission data
88 were analyzed to investigate the meteorological condition PLAM index identification
89 method for forecasting wide-range low visibility and fog-haze.

90

91 **2.1 Analysis on wet-equivalent potential temperature θ_e features of uniform air** 92 **mass**

93 Air quality and meteorological condition impacts are closely related. Usually different
94 air mass structures can lead to significant difference of meteorological conditions.
95 Studies pointed out that, aiming at the impact on air quality, it is very important to
96 analyze and distinguish what kind of air mass controls and affects the local area,
97 identify the differences of atmospheric aerosol features of the air masses in different
98 types including maritime air mass, continental air mass or polar air mass etc., and
99 consider the identification of stagnant air mass. The property of wet-equivalent
100 potential temperature θ_e can be used to distinguish the types of air masses, because θ_e

101 includes dry and wet adiabatic processes, lifting condensation and sinking and other
 102 dynamic and thermodynamic processes in atmosphere, having the property of
 103 conserving and being able to be tracked and identified. The equation of wet-equivalent
 104 potential temperature is:

$$105 \quad \theta_e = \theta \exp\left[\left(\frac{Lw}{C_p T}\right)\right] \quad (1)$$

$$106 \quad \text{where: } \theta \text{ is potential temperature: } \theta = T \left[\left(\frac{1000}{P} \right)^{\frac{R_d}{C_p}} \right] \quad (2)$$

107 the unit of θ and θ_e is K . w , C_p , L , R_d , P and T are mixing ratio,
 108 constant-pressure specific heat ($C_p=1.005 \text{ J}\cdot\text{g}^{-1}\cdot\text{degree}^{-1}$), latent heat of
 109 condensation of water vapor ($L = 2500.6 \text{ J}\cdot\text{g}^{-1}$), gas constant ($R_d = 2.87\cdot 10^{-1}$
 110 $\text{J}\cdot\text{g}^{-1}\cdot\text{degree}^{-1}$), air pressure and temperature, respectively.

111

112 **2.2 Parameterized method of diagnosing and forecasting atmospheric process**

113 The interactions and mutual effects of atmospheric micro-physical process and
 114 large-scale process as well as the different scales of process are very complicated in
 115 the transient of cloud and fog physical process as well as the atmospheric pollution
 116 process. The meaning and main idea of the parameterized method is to connect the
 117 non-linear relationship that is difficult to describe in the processes of different scales
 118 with a parameterization scheme. Studies (Kuo, 1961; Kuo,1965; Kuo, 1974) have
 119 shown that the micro-processes in cloud physics can be described in a
 120 parameterization scheme with the large-scale observations. Based on the Lagrangian
 121 method the variation of fluid particle group going with time can be followed, i.e.,
 122 identifying the “stagnant and less changing” state of air masses. In the atmospheric
 123 particle movement, the individual change of wet-equivalent potential temperature
 124 (spatial-temporal total derivative) gets to a small value or zero, meaning little
 125 changes. Therefore, according to the identification of the “stagnant and less
 126 changing” property of wet-equivalent potential temperature of air masses, i.e., the
 127 basic physical process of $\frac{d\theta_e}{dt} \approx 0$, the possible varying trend of air quality of the

128 “stagnant and less changing” air masses can be diagnosed and predicted. The
 129 recently developed air quality diagnosis of parameterized meteorological conditions
 130 (Yang, et al., 2009 ; Zhang, et al., 2009; Wang, et al., 2012) PLAM index is described
 131 as follows:

$$132 \quad \text{PLAM}_0 = d\theta_e/dt \cong \theta_e \frac{f_c}{C_p T} \quad (3)$$

133 θ_e is wet-equivalent potential temperature given out by Eq.(1). f_c is wet air
 134 condensation rate:

$$135 \quad f_c = f_{cd} / \left[\left(1 + \frac{L}{C_p} \frac{\partial q_s}{\partial T} \right)_p \right] \quad (4)$$

136 f_{cd} is dry air condensation rate:

$$137 \quad f_{cd} = \left[\left(\frac{\partial q_s}{\partial P} \right)_T + \gamma_p \left(\frac{\partial q_s}{\partial T} \right)_p \right] \quad (5)$$

$$138 \quad \gamma_p \text{ is dry-adiabatic lapse rate: } \gamma_p = \frac{R_d}{C_p} * \frac{T}{P} \quad (6)$$

139 q_s is specific humidity. The meanings of other variables are the same as the
 140 above-mentioned.

141 The Eq.(3) shows that the parameterized method based on the spatial-temporal
 142 variation of wet-equivalent potential temperature of air masses has practical application
 143 prospect in analyzing, diagnosing and forecasting the changes of air quality. The
 144 objective of this paper is to further discuss the impact and identification of PLAM₀
 145 index to aerosol pollution concentration accumulative increase and atmospheric
 146 fog-haze weather, and moreover study the possibility of using the parameterized
 147 method to improve the diagnosing and forecasting capability to large-scale disastrous
 148 fog-haze weather.

149

150 **2.3 Contribution and impact of atmospheric emission on PLAM index**

151 Considering the diagnosis and forecasting analysis of atmospheric fog-haze which is
 152 closely related to atmospheric aerosols (such as fine particle PM_{2.5} etc.), it is very
 153 important to integrate the effect of the initial meteorological conditions PLAM₀ and

154 emission contribution. In order to integrate the initial meteorological condition related
 155 to atmospheric pressure, temperature, humidity, condensation, etc. with the
 156 contribution of the pollutant emission factor p in the atmosphere, the identification
 157 parameter was expressed by Eq. (7) (Wang et al., 2012) :

$$158 \quad \text{PLAM_haze} = \text{PLAM}_0 \times p \quad (7)$$

159 This factor p further expands the application of PLAM index and investigates the
 160 description of the function and impact of the index by emissions in the forming and
 161 developing process of regional wide-range fog-haze event, namely PLAM_haze
 162 (abbreviated as PLAM/h). Thus, analysis on the latest emission research results as of
 163 2010 is introduced including industry, energy source, transportation, anthropogenic
 164 emission source combined $E_{\text{PM}_{2.5}}$ (Unit: tons *10)(Figure 1a). It is seen from Figure 1a
 165 that the high-value zones from industry, energy source, transportation and
 166 anthropogenic emission source in the North China region involve ① the central and
 167 southern part of Hebei (including Beijing and Tianjin), ② the central and western part
 168 of Shandong, ③ the central part of Henan, ④ the eastern part of Hubei, ⑤ the Yangtze
 169 River delta and ⑥ the eastern part of Sichuan (the Chengdu Plain). All these
 170 high-value emission sources have significant impacts on the fog-haze weather in North
 171 China and cannot be underrated.

172 To quantify the impact of emission in PLAM index, the probability of its impact
 173 on the surrounding area satisfies the normal distribution, that is, by separating the
 174 impacts of meteorological condition and emission on the surrounding part, it is always
 175 isotropic and the impact probability of high emission center area is higher than that of
 176 the surrounding area. As a result, the emission impact satisfies the form of
 177 2-dimensional probability distribution, and the integral probability density function that
 178 falls into the surrounding limited area x, y plane (s) is as follows:(Wang et al, 1985 ;
 179 Neumann et al., 1978):

$$180 \quad P'(s) = \iint_s f(x, y) dx dy = 1 - \exp(-\gamma^2/2) \quad (8)$$

181 where γ is the standardized (normalized) grade of the emission source intensity in the
 182 concerned forecasting area, $\gamma \in (0, 1)$, defined as $\gamma = (E - E_{\min}) / (E_{\max} - E_{\min})$, where E_{\max}
 183 and E_{\min} are the maximum value and minimum value of the emission E in the specified
 184 season of the studied impact region (North China). In other words, the exponential

185 growth rate with emission impact is $P = 1 + P'$. Then, the impact of emission on the
186 increase value of fog-haze is taken into account, and the Eq. (3) can be formulated into:

187
$$\text{PLAM}/h = \theta_e \frac{f_c}{C_p T} \times p(\gamma) \quad (9)$$

188 **3 Results and Discussion**

189 **3.1 Analysis on PLAM index medium emission contribution features**

190 Studies pointed out that emission does not change very much in certain fixed temporal
191 scales (such as a month or a season) in the same area, but differs greatly in different
192 places. To analyze the contribution of regional emission on the low visibility weather
193 like fog-haze, the comparable standardized emission intensity (γ) in the regional and
194 seasonal period was calculated based on the meteorological observation data in
195 different places and different time periods. Figure1a presents the distribution of high
196 resolution emission lists. Figure1b is the standardized distribution of emission list in
197 the North China region based on Figure1a. From Figure 1b, it can be seen that ①
198 Beijing, Tianjin and the central and southern part of Hebei, ② the west of Shandong,
199 ③ the central part of Henan, ④ the eastern part of Hubei, ⑤ the Yangtze river delta
200 and ⑥ the east of Sichuan remain to be the significantly concentrated high emission
201 regions, whose circular or oval-shaped distribution characteristics are clearly seen.
202 Taking the rarely-seen large-range heavy fog-haze weather event over Beijing and the
203 North China region on 26 February 2014 as an example, the difference by considering
204 and ignoring the emission contribution in PLAM index is discussed. Figure1c and d
205 show the PLAM index distribution under the condition of considering and ignoring the
206 emission in North China at 08:00 (UTC+8) 26 February 2014. It is seen from the figure
207 that under the condition without considering the emission impact (Figure1c) the
208 distribution centers of PLAM index are: Hebei, Beijing-Tianjin region in North China;
209 southern Hebei, northern Henan; western Hubei and northern Sichuan. The PLAM
210 indices are 120, 160, 160 and 80 (Figure.1c) respectively. Figure1d shows PLAM/h
211 distribution with the emission impact. The above-mentioned four PLAM/h index high
212 value zones are 180, 180, 180 and 160, respectively. The PLAM/h value increases
213 along with the significant expansion of high-value (the green oval-shaped circle in the
214 figure).

215 To further discuss the difference, Figure2 displays the correlation analysis of 24
216 h forecasting and visibility of PLAM/h index at 673 stations in North China on

带格式的：突出显示

217 26 February 2014. For the convenience to compare, the overlap of the correlati
218 on distributions of PLAM/h and visibility under the condition of including and
219 excluding emission factors is given out. The considered emission in Figure 2 is
220 expressed by blue triangle while the ignored emission is marked with red circl
221 e -- yellow filled circle. The correlation fitted lines are respectively marked by
222 red solid line and yellow dashed line. It is seen from Figure 2 that the reasona
223 ble correlation exists between PLAM/h and visibility on 26 February 2014 regar
224 dless of emission contributions. However, determination coefficient (R^2) is increa
225 sed from 0.3675 to 0.3887 when emissions are considered, indicating the import
226 ance of inclusion of emission in PLAM/h.

删除的内容: black dashed line

带格式的: 字体: (默认) Times
New Roman, 小四

删除的内容: correlation

227

228 It is noted that in the low-value visibility range ($Vis < 10\text{km}$), the PLAM/h index
229 value without emission impact shifts towards low-value zone clearly. Comparatively,
230 the closer to the high-value zone of visibility, the more the two types of symbols tend
231 to overlap, which suggests that, without emissions, the predictive value of PLAM/h
232 index will be smaller and its correlation with visibility will be reduced, deviating the
233 fitted low-value zone line.

234 In summary, the above analyses on the regional PLAM/h distribution (Figure 1)
235 and the correlation distribution of PLAM/h and visibility (Figure 2) all indicate that
236 with the combined impact of meteorological condition and emission factors, the
237 description capability of PLAM/h index increases significantly with the index value
238 expanding to the high-value zone; the PLAM/h index including the emission has
239 obvious impact on improving the capability of diagnosing and identifying the heavy
240 fog-haze weather.

241

242 3.2 Analysis on seasonal characteristics of PLAM/h index and visibility 243 correlation

244 Figure 3 separately presents distribution of fog-haze weather in the typical heavy
245 fog-haze process cases in four seasons, including the PLAM/h (a) and visibility (b) of
246 the 14 April 2011 spring case, the PLAM/h (c) and visibility (d) of the 26 July 2008
247 summer case, the PLAM/h (e) and visibility (f) of the 30 October 2011 autumn case
248 and the PLAM/h (g) and visibility (h) of the 7 January 2011 winter case.

249 In spring, the PLAM/h index low-value zone on 14 April 2011 is mainly in the

252 North China region. 3/4 regional PLAM/h < 70 in the whole region. The
253 meteorological condition is good for pollutants to diffuse. There is a weak PLAM/h
254 relatively high-value zone across the central Henan, southern Hebei, Beijing-Tianjin
255 and northern Hebei, which is PLAM/h ≥ 80. Besides, there is another high-value zone in
256 the coastal parts of Bohai Sea, corresponding to the sea fog prone area in the southern
257 part of North China. The PLAM/h high value matches with the low-value zone of
258 visibility whilst the large-range PLAM/h low-value zone goes with the high-value zone
259 of visibility.

260 In Summer, the 08:00(UTC+8) 26 August 2008 case shows that the North China
261 region is a large-scale PLAM/h high-value zone, whose center distributes in
262 north-south banding shape: ① East of Taihang Mountains in Henan province to
263 southern Hebei (PLAM/h value is 120 and the highest even gets to 200), ② Beijing
264 and central Hebei (PLAM/h value is 120-140), ③ the Jing-Jin-Tang (Beijing, Tianjin,
265 Tangshan) region (PLAM/h value is high up to 120-240) and ④ the west-southern
266 Shandong (PLAM/h value reaches 140-200) are four remarkable banding high value
267 centers. Corresponding to the wide-range low visibility low value zones, the visibility
268 in most parts is lower than 10 km, of which the visibility from Henan to southern Hebei
269 is lower than 4 km. The Beijing-Tianjin region has the visibility of 4-8 km only. So,
270 PLAM/h index has significant effect on diagnosing and identifying the summer
271 fog-haze weather in North China.

带格式的: 突出显示

272 North China usually has clear and refreshing autumn weather. But in recent years,
273 heavy fog-haze weather events appear more and more frequently in autumn. To
274 examine the identifying capability of PLAM/h index in the typical autumn heavy
275 fog-haze case, we analyze the rarely seen heavy fog-haze pollution process that
276 happened in North China on 30 October 2011. According to Figure 3g and 3h, the
277 high-value PLAM/h index in the fog-haze area in North China assumes in the
278 north-south trend parallelized to the regional distribution of three large-scale bands (3g)
279 and PLAM/h > 200-240, of which the three high-value PLAM/h bands are parallel
280 to the Taihang Mountains in North China, orderly arranged along the line of the boundary
281 between Shanxi and Hebei-southern Liaoning (dotted line in the figure) and being
282 greatly consistent with the banding distribution of the fog-haze and low visibility areas
283 in North China (Figure 3h). The large scope of PLAM/h low-value zone, PLAM/h <
284 20-50, in the western and northern parts of North China agrees with the high-value

285 visibility zone with $Vis > 20\text{km}$. Therefore, PLAM index has the characteristics of
286 weather-scale banding distribution similar to the distribution of weather systems.

287 One heavy fog-haze process rarely seen in history appeared in North China in the
288 first-half month of January 2013. This is a typical winter heavy fog-haze case, whose
289 PLAM/h index is significantly high, indicating the contribution of meteorological
290 condition to the enhancement and persistence of this large-range fog-haze process is
291 dominating. PLAM/h index high-value zone blankets the Beijing-Tianjin, the east to
292 Taihang Mountains to the most part of North China which is to the south of Yanshan
293 Mountains. The banding fog-haze weather area in the southwest-northeast trend
294 extends eastward into the southern part of Liaoning. Corresponding to the
295 southwest-northeast trend banding high-value zone of PLAM/h index (Figure 3g), the
296 visibility is the accordant banding low-value distribution area (Figure 3h)

297 The seasonal results analysis of PLAM/h index shows its characteristics linkage
298 with weather-scale system in each season. The weather-scale high-value PLAM/h zone
299 agrees with the low-value visibility area, which indicates the regional distribution of
300 PLAM/h index is indicative of diagnosing, identifying and forecasting the large-range
301 fog-haze area in four seasons in North China.

302 Figure 4 reveals the correlation of PLAM/h index and visibility in different
303 seasons which is calculated by Eq. (9) according to the 2009 daily observation data in
304 Beijing. As the seasonal features related to aerosol pollution in North China are
305 different from the seasonal features divided according to temperature elements, the
306 selected representative stations are slightly different. For the analysis of this paper, the
307 season from July to August is defined as rainy season or summer and from November
308 to the next February is winter in North China. Spring and autumn are two transition
309 seasons, taking March to June and September to October respectively. In Figure 4a the
310 chosen period of winter includes January-February and November-December of
311 Beijing (BJ) and Zhengzhou (ZZ), there are totally 240 groups of observation record.
312 In Figure 4b there are totally 248 groups of observation records chosen for the summer
313 July-August of Beijing (BJ), Zhengzhou (ZZ), Taiyuan (TY) and Jinan (JN). Figure 4c
314 involves 122 groups of records from Beijing (BJ) for the season of spring March-June.
315 Figure 4d contains 122 groups of observation records for the autumn
316 September-October of Beijing (BJ) and Zhengzhou (ZZ). It is seen from the figures
317 that:

- 318 1) The variation of air quality meteorological condition PLAM/h index is significantly
319 correlated to the visibility observation (Vis) in Beijing and the **determination**
320 coefficients (R^2) are 0.8587 (winter), 0.8009 (summer), 0.7617 (spring) and 0.9552
321 (autumn), respectively, with all significance levels exceeding 0.001.
- 322 2) In winter (Figure 4a), with the low-value meteorological condition index, when
323 $PLAM/h < 80$, $Vis > 25$ km; when high value of PLAM/h gets up to 150-350, the
324 observed visibility trend gets worse with $Vis < 10$ km. Different from winter,
325 during the low-value meteorological condition index in summer, when $PLAM <$
326 **150**, $Vis \geq 10$ km; when the PLAM high value rises to 150, the observed visibility
327 becomes worse and $Vis < 5$ km (Figure 4b). This means that PLAM/h has
328 significant capability to describe optimal or inferior visibility, and, moreover, its
329 seasonal difference is great. This finding is consistent with the climate observation
330 result that the aerosol concentration high value in summer appears at the same pace
331 with low visibility(Wang, 2006).
- 332 3) Figure 4 shows that the correlations in the two transition seasons are noticeably
333 different. The correlation features in spring are similar to those in summer while
334 the autumn features are like winter's. But during the transition seasons, spring and
335 autumn, the threshold value deduced from the diagnosis of PLAM/h to heavy
336 fog-haze pollution is lower, that is, when the meteorological condition index
337 PLAM/h gets to 150, visibility is with very low value, even $Vis < 5$ km.

删除的内容: correlation

带格式的: 字体: (默认) Times
New Roman, 小四, 突出显示

删除的内容: 100

删除的内容: <

338 In summary, the above analyses indicate that PLAM/h is capable to describe the
339 changes of visibility, and also capable of distinguishing the seasonal differences very
340 well. The seasonal threshold difference resulting from the diagnosis of PLAM/h to
341 heavy fog-haze pollution is indicative of quantitatively identifying and diagnosing the
342 appearance of fog-haze pollution.

343

344 3.3 PLAM index and related features of visibility area

345 Figure 5 shows the regional correlation between PLAM/h index and visibility which is
346 obtained by calculating the 1006 groups of observation samples collected from January
347 2009 to December 2012. **the icon for 0-100%, drawing the R^2 value magnified by 100**
348 **in Fig.5**. The regional distribution of the correlation with significance level exceeding
349 0.001 is also shown. The figure indicates that most part of North China is the
350 high-value zone $> 80\%$, of which one high-value zone is located in Shanxi, most

带格式的: 字体: (默认) Times
New Roman, 小四, 突出显示

带格式的: 字体: (默认) Times
New Roman, 小四, 突出显示

带格式的: 突出显示

354

355

356 Mountains in North China as well as the distribution of high emission areas in southern
357 Hebei and northern Hubei (Figure 1b); another high correlated zone which sits in
358 Beijing-Tianjin and the Bohai Bay rim is possibly related to the weather condition of
359 the more fog-haze “back-flow” of the easterly wind in North China. These analyses
360 suggest that the North China PLAM/h and index features are significantly correlated to
361 visibility, the high correlation area with significance level exceeding 0.001 is likely
362 related to the regional distribution of meteorological condition of heavy fog weather in
363 North China and the distribution of regional emission high-value zone in North China.

364

365 **3.4 Application of PLAM/h index in fog-haze forecasting**

366 **3.4.1 The 20-26 February 2014 winter case analysis**

367 Applying the PLAM/h index developed in this paper, 24 h forecasts of visibility with
368 PLAM/h are conducted for one historically rarely-seen winter heavy fog-haze process
369 in North China during the last half of February 2014 (20-26 February 2014). During
370 the test, the NRT data of more than 670 stations in the North China region are adopted
371 to analyze the correlation between PLAM/h index 24 h forecasts and visibility
372 observation. Figure 6a and b reveal the correlation analysis results of PLAM/h index
373 24 h forecasts and observed visibility respectively at 08:00 (UTC+8) 20 and 08:00
374 (UTC+8) 22 February 2014. Table 1 lists the correlation of daily PLAM/h index 24 h
375 forecasts and visibility during the whole process of the regional heavy fog-haze event
376 over North China in 20-26 February 2014 as well as the number of stations that are
377 involved in the test.

带格式的: 突出显示

378 From Figure 6 and Table 1 it can be seen the daily determination coefficients (R^2)
379 are 0.6529, 0.5424, 0.6047, 0.6040, 0.4550 and 0.3887, respectively; the significance
380 levels all pass 0.001, which means their correlation is very good.

带格式的: 字体: (默认) Times
New Roman, 小四, 突出显示

删除的内容: correlation

381

382

383 **3.4.2 The 19-22 July 2013 summer case analysis**

384 To further investigate the forecasting capability of summer PLAM/h index to the
385 fog-haze area distribution, forecast application and testing analysis of one heavy
386 fog-haze pollution process in North China in summer 19-22 July 2013 are carried out.
387 On 19 July, extremely heavy fog emerged in the day time over Beijing, just as night

389 had fallen. It was very dark with local visibility less than 5 m. Figure 7a and b reveal
390 the correlation analysis result of PLAM/h index 24 h forecast and visibility during the
391 | polluting process in the North China region respectively at 08:00 (UTC+8) 20 and 22
392 July 2013. Table 2 presents the correlation of daily PLAM/h index 24 h forecast and
393 visibility during the whole process of the regional heavy fog-haze event over North
394 China in 19-22 July 2013 as well as the number of stations that participate in the
395 | forecasting test. From Figure 7 and Table 2, the daily determination coefficients (R^2)
396 respectively are 0.4988, 0.4826, 0.5416 and 0.5263, and all their significance levels
397 exceed 0.001.

带格式的: 字体: (默认) Times
New Roman, 小四, 突出显示

删除的内容: correlation

398 The above analyses indicate that the PLAM/h index 24 h forecasts and visibility
399 observations of the large-range samples in different winter and summer over North
400 China all have higher correlations. This result illustrates the PLAM/h index would have
401 good practical application prospect in forecasting the regional large-scale fog-haze
402 weather in North China.

403

404 3.4.3 The 12 March 2014 fine weather case analysis

405 In order to investigate the analysis and identification capability of PLAM/h to
406 the fine and sunny weather without fog or haze, the correlation between PLAM/h and
407 visibility in a wide range of fine weather has been carried out. As an example, Figure
408 8a and b reveal the correlation analysis of the regional PLAM/h distribution and
409 PLAM/h index 24 h forecasts on 12 March 2014.

410 It is seen from Figure 8a that most part of North China has low-value PLAM/h
411 < 60 (blue area in the figure). The meteorological condition PLAM/h index
412 distribution displays that large area of North China lies in the area with the
413 meteorological condition extremely favorable for atmospheric dispersion. Beijing is
414 under blue sky with clouds. The PLAM/h index forecasts of Beijing and Baoding
415 (Hebei) are 53 and 29 respectively. From daytime to evening on 12 March, the $PM_{2.5}$
416 value of Beijing urban area is reported to be 21-35 $\mu\text{g}/\text{m}^3$.

417

418 Figure 8b is the correlation analysis of PLAM/h index 24 h forecasts and
419 observed visibility at 677 stations in North China on 12 March 2014, which was made
420 | based on real-time data. It can be seen that the determination coefficient (R^2) gets to
421 0.412 and the significance level passes 0.001 averagely. On 13 March 2014, Beijing

删除的内容: correlation

带格式的: 字体: (默认) Times
New Roman, 小四, 突出显示

424 continues to enjoy the clear weather with blue sky and clouds, so air quality is
425 excellent. The $PM_{2.5}$ value of Beijing urban area still remains at high level of
426 $22-37\mu\text{g}/\text{m}^3$. The above analysis indicates that for large-scale fine weather or
427 low-visibility heavy pollution weather, PLAM/h index has the strong capability of
428 identifying, analyzing and forecasting.

429

430 **4. Conclusions**

431

432 PLAM – A meteorological pollution Index for air quality has been developed and used
433 in NRT air quality forecasts, by considering both meteorology and pollutant emissions.
434 Based on the emission diagnosing model of 2-dimensional probability density function,
435 the paper has extended the parameterized description of original PLAM, applying it in
436 the diagnosis and forecasting of the variation and distribution of wide-range regional
437 low-visibility fog-haze intensity and achieving satisfactory results. The contrast
438 analysis with or without the emission impact indicates that meteorological condition
439 and emission factor jointly play the role in expanding PLAM towards high-value zone.
440 This means that PLAM/h index involving emission has significant effect on improving
441 the capability of diagnosing and forecasting heavy fog-haze weather in North China.

442 The variation of air quality meteorological condition index PLAM/h is
443 significantly correlated to the regional visibility observations in North China. The
444 **determination** coefficients of winter, summer, spring and autumn are 0.8557 (winter),
445 0.8009 (summer), 0.7617 (spring) and 0.9552 (autumn), respectively and their average
446 significance level goes beyond 0.001.

带格式的: 字体: (默认) Times
New Roman, 小四, 突出显示

删除的内容: correlation

447 The correlation analysis of index and visibility regional distributions indicates that
448 the high correlation zones respectively lie in Jing-Jin-Ji (Beijing, Tianjin, Hebei),
449 Bohai Bay rim, southern Hebei and northern Hubei. This indicates that PLAM/h index
450 is related to the distributions of the North China weather system and the heavy fog
451 occurrence region as well as the distribution of emission high value zones, which is
452 indicative to diagnose and identify the regional distribution of the fog-haze frequently,
453 hit areas.

454 The analyses on typical high pollution cases of spring, summer, autumn and winter
455 suggest that PLAM/h index regional distribution is related to the banding distribution
456 features of weather-scale systems in different seasons. The weather-scale high-value
457 PLAM/h areas correspond to the low-visibility areas, indicating the PLAM/h index has

459 the diagnosing, identifying and forecasting capability to the wide-range fog-haze areas
460 and their seasonal differences in North China.

461 Although winter is different from summer, the PLAM/h index 24 h forecasts and
462 visibility observations from the weather stations of North China, including wide-range
463 fine weather and the low-visibility heavy pollution weather, all have high correlations.
464 This indicates the PLAM/h index has good identifying, analyzing and forecasting
465 capabilities. These conclusions show that the PLAM/h index will have good practical
466 application prospect in forecasting the large-scale fog-haze areas and their seasonal
467 differences in North China.

468

469 ***Acknowledgements***

470 This work was funded by the National Key Foundation Study Developing
471 Programm (2011CB403404,2011CB403401), National Key Technology R&D Program
472 (Grant no. 2014BAC16B01) National Natural Science Foundation of China under
473 Grant (No. 41275167, No. 41275007) and CMA Innovation Team for Haze-fog
474 Monitoring and Forecasting

475

476 References

477 Gong, S.L., Barrie, A., Blanchet, J.P., Salzen, K. N, Lohmann, U., Lesins, G.,
478 Spacek, L.,Zhang, L.M., Girard, E., Lin, H., Leitch, R., Leighton, H., Chylek, P.,
479 Huang, P.: Canadian aerosol module: a size-segregated simulation of atmospheric
480 aerosol processes for climate and air quality models 1. Module development J.
481 Geophys. Res. 108, 4007-4015, 2003.

带格式的: 突出显示

482 Honore ´, C., Rouil, L., Vautard, R.: Predictability of European air quality:
483 Assessment of 3 years of operational forecasts and analyses by the PREV'AIR system.
484 J. Geophys. Res.,113: D04301,4302-4310, 2008.

删除的内容: .

带格式的: 突出显示

485 Kassomenos, P., Papaloukas, C., Petrakis, M., Karakitsios, S.: Assessment and
486 prediction of short term hospital admissions: the case of Athens, Greece. tmos. Environ.
487 42 (30), 7078-7086, 2008.

488 Kuo,H.L.: Convective Weather in Conditionally Unstable Atmosphere, Tellus, 13,
489 441-459, 1961.

490 Kuo,H.L.: On Formation and Intensification of Tropical Cyclone through Latent
491 Heat Release in Cumulus Convection, J .Atmos. Sci 22,40-23,1965.

492 Kuo,H.L.:Further Studies on the Parameterization of the Influence of Cumulus
493 Convection in Large-scale Flows, J. Atmos. Sci. 31,1232-1240, 1974.

494 Li, Y., Wang, W., Wang, J.Z., Zhang, X.L., Lin, W.L., Yang, Y.Q.: Impact of air
495 pollution control measures and weather conditions on asthma during the 2008 Summer
496 Olympic Games in Beijing. Int. J. Biometeorol.. http://dx.doi.org/
497 10.1007/s00484-010-0373-6, 2010.

498 McKeen, S.: Evaluation of several real-time PM2.5 forecast models using data
499 collected during the ICARTT/NEAQS 2004 field study, J. Geophys. Res. 112: D10S20,
500 DOI: 10.1029/2006JD007608,2007.

带格式的: 字体: 非加粗, 突出显示

带格式的: 突出显示

带格式的: 默认段落字体, 字体:
(默认) Times New Roman, 小四,
字体颜色: 黑色, 图案: 清除, 突出显示

501 Moran, M.D.:on particulate matter formation in the Mediterranean Region. In
502 Proceedings of the 30th NATO/SPS ITM on Air Pollution Modelling and Its
503 Application, (San Francisco), 2009.

带格式的: 字体: (默认) Times
New Roman, 小四, 字体颜色: 黑
色, 图案: 清除, 突出显示

带格式的: 字体: (默认) Times
New Roman, 小四, 字体颜色: 黑
色, 图案: 清除, 突出显示

504 Neumann C. J.,Mandal, G. S.: Analog forecasting methods of tropical cyclones in
505 India ocean. Indian J Met. Geophys.,29(3):487-500,1978.

带格式的: 字体: (默认) Times
New Roman, 小四, 字体颜色: 黑
色, 图案: 清除, 突出显示

506 Rigby, M., Toumi, R.: London air pollution climatology: indirect evidence for
507 urban boundary layer height and wind speed enhancement. Atmos. nviron. 42 (20),
508 4932-4947. 2008.

509 Wang, J. Z., Gong, S. L., Zhang, X. Y.,Yang,Y. Q. Hou, Q., Zhou,C.H., and

511 Wang, Y.Q.: A parameterized method for air-quality diagnosis and its applications.

512 Adv Meteorol. [Article ID 238589: 1-10](#),doi:10.1155/2012/238589, 2012.

带格式的: 字体: (默认) Times
New Roman, 小四, 突出显示

513 Wang,J.I.,Liu, X.I.: The Discuss on relationship between visibility and mass
514 concentration of PM_{2.5} in Beijing, Acta Meteorlo Sin, 64 (2) ,221-228,2006.

515 Wang J.Z., Neumann, C. J.: A Markov-type analogmedel for prediction of
516 typhoon motion in Northwestern Pacific, Scientia Sinica (Series B),28(5):517-526,

517 1985. Wang,J.Z., Wang, Y.Q., Liu, H., Yang, Y.Q., Zhang,X.Y., Li, Y., Zhang, Y.

518 M., Deng, G.:Diagnostic identification of the impact of meteorological conditions on

519 PM_{2.5} concentrations in Beijing Atmospheric Environment, 81 158-165, 2013.

520 Wang, J.Z., Yang, Y.Q., Zhang, G.Z., Yu, S.Q.: Climatic trend of cloud amount
521 related to the aerosol characteristics in Beijing during1950-2005, Acta Meteorol. Sin.

522 24 (6), 762-775, 2010.

523 Wang J. Z., Xu, X. D., Yang, Y.Q.: A studyof characteristics of urban visibility
524 and fog in Beijing and the surrouding area(in Chinese), Journal of Applied
525 Meteorological Science Suppl 13: 160-168, 2002.

526 Yang,Y.Q., Wang,J. Z., Hou, Q., Wang,Y. Q.: A Plam Index for Beijing
527 Stabilized Weather Forecast in Summer Over Beijing. Journal of Applied

528 Meteorological Science 20, 649-655, 2009.

带格式的: 突出显示

529 Zhang, X. Y., Sun, J. Y., Wang, Y. Q., Li, W. J., Zhang, Q., Wang, W. Z., Qian, J.

530 N.,Cao, G. L., Wang, J. Z., Yang, Y. Q., Zhang, Y. M.: Factors contributing to haze

531 and fog in China (in Chinese), Chin Sci Bull (Chin Ver), 58: 1178-1187,doi:

532 10.1360/972013-150,2013.

533 Zhang, X.Y., Wang, Y.Q., Lin, W.L., Zhang, Y.M., Zhang, X.C., Gong, S.L.,

534 Zhao, P., Yang, Y.Q., Wang,J.Z., hou, Q., Zhang, X.L., Che, h. Z., Guo, J.P., Li, Y.:

535 Changes of atmospheric composition and optical properties over Beijing 2008 Olympic

536 Monitoring Campaign. Bull. Am. Meteorol. Soc. 90 (11), 1633-1649, 2009.

537

538

539

540

541

542

543
544
545
546
547
548
549
550
551
552
553
554
555
556
557
558
559
560
561
562
563
564
565
566
567
568
569
570
571
572
573
574
575

Figure captions

Figure 1 High resolution emission list E distribution (a) and its regional emission standardized list γ (b); PLAM index distribution with ignoring (c) and considering (d) the emission condition in North China at 08:00 (UTC+8) 26 February 2014

Figure 2 Correlation analysis of PLAM and visibility considering and not considering emission factors on 26 February 2014

Figure 3 The cases for PLAM/h (a) and visibility (b) of the 14 April 2011 , PLAM/h (c) and visibility (d) of the 26 July 2008, PLAM/h (e) and visibility (f) of the 30 October 2011 and PLAM/h (g) and visibility (h) on 7 January 2011

Figure 4 Correlation analysis of PLAM/h index and visibility in winter (a), summer (b), spring (c) and autumn (d)

Figure 5 the regional correlation between PLAM/h index and visibility obtained by calculating the 1006 groups of observation samples collected from January 2009 to December 2012. The regional distribution of the correlation with significance level exceeding 0.001

Figure 6 the correlation analysis results of PLAM/h index 24 h forecasts and observed visibility respectively at 08:00 (UTC+8) 20(a) and 08:00 (UTC+8) 22(b) February 2014

Figure 7 Correlation analysis of the regional PLAM/h index 24 h forecasts and visibility during the whole period of pollution in North China respectively at 08:00(UTC+8) 20(a) and 08:00(UTC+8) 22 July 2014(b)

Figure 8 distribution of PLAM/h in North China (a)and the correlation analysis of PLAM/h index 24 h forecasts and observed visibility in North China for 8:00(UTC+8) March 12, 2014 (b)

Table 1 Correlation of daily PLAM/h index 24 h forecasts and visibility during the whole process of the regional heavy fog-haze event over North China in 20-26 February 2014

刪除的內容: .
.
.
.
.
.
.
.
.

586

587

588

589

590

591

592

593

594

595

596

597

598

599

600

Table 2 Correlation of daily PLAM/h index 24 h forecasts and visibility during the whole process of the regional heavy fog-haze event over North China in 19-22 July 2013

Forecast time	determination coefficient (R ²)	Station number
08 :00(UTC+8) 20 Feb.	0.6529	674
08 :00(UTC+8) 21 Feb.	0.5424	668
08 :00(UTC+8) 22 Feb.	0.4634	669
08 :00(UTC+8) 23 Feb.	0.6047	676
08 :00(UTC+8) 24 Feb.	0.6040	673
08 :00(UTC+8) 25 Feb.	0.4550	678
08 :00(UTC+8) 26 Feb.	0.3887	673

删除的内容: Correlaton

带格式的: 字体: (默认) Times New Roman, 六号, 法语(法国)

删除的内容:

601

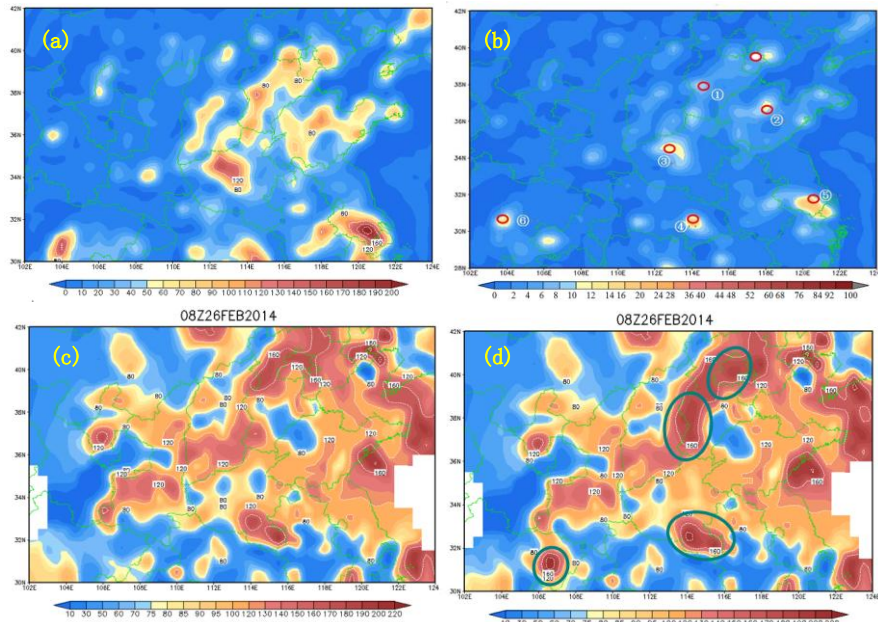
Forecast time	determination coefficient (R ²)	Station number
08 :00(UTC+8) 19 Jul.	0.4988	682
08 :00(UTC+8) 20 Jul.	0.4826	683
08 :00(UTC+8) 21 Jul.	0.5416	685
08 :00(UTC+8) 22 Jul.	0.5263	181

带格式表格

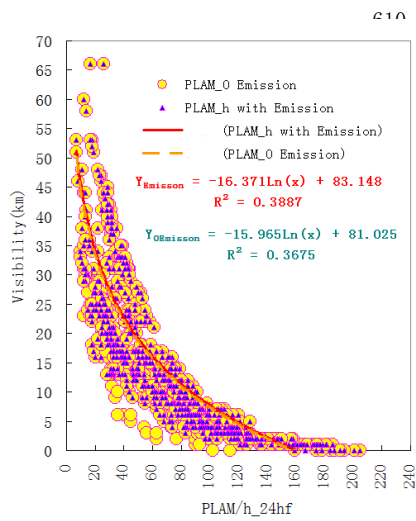
带格式的: 字体: (默认) Times New Roman, 六号, 法语(法国), 突出显示

删除的内容: Correlaton

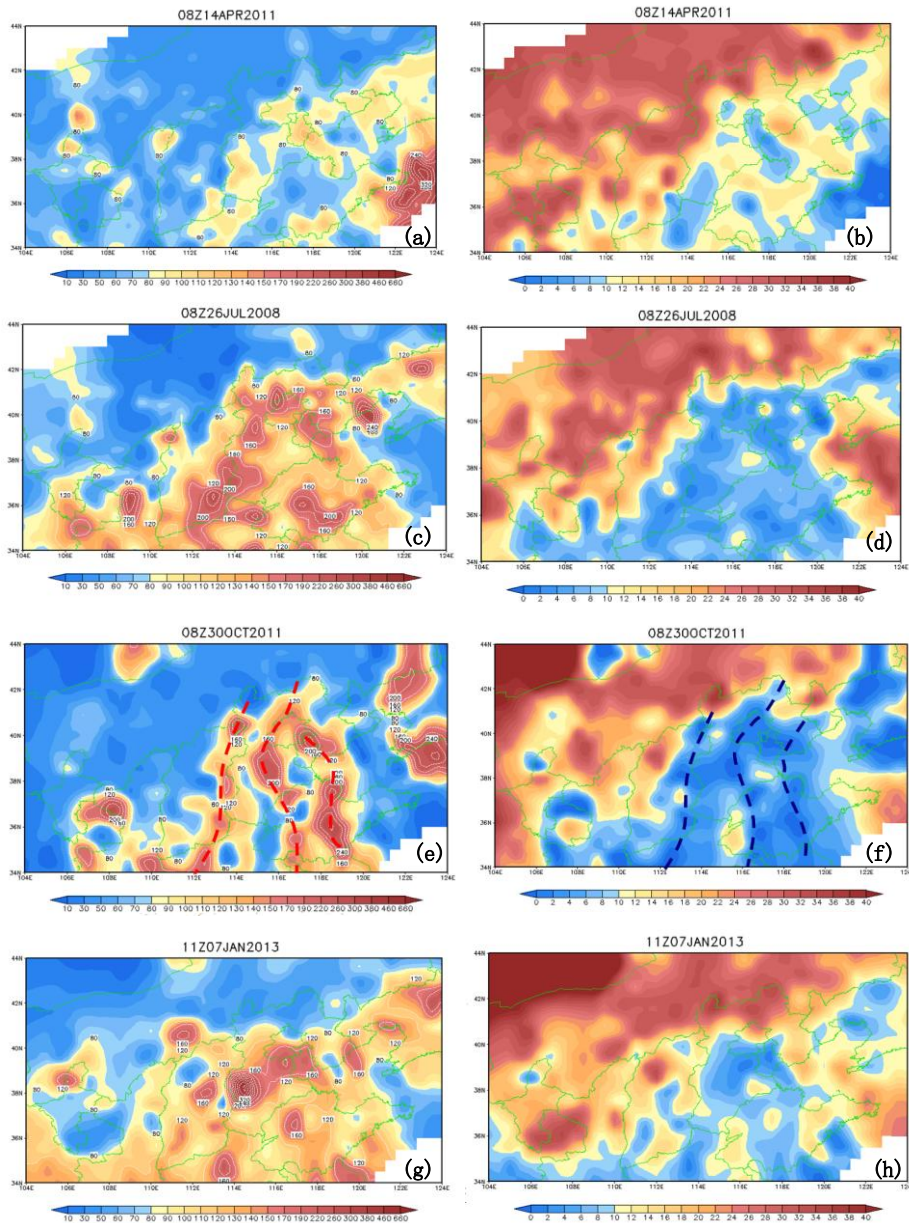
605 Figure 1 High resolution emission list E distribution (a) and its regional emission
 606 standardized list γ (b); PLAM index distribution with ignoring (c) and considering (d)
 607 the emission condition in North China at 08:00(UTC+8) 26 February 2014



608 Figure 2 Correlation analysis of PLAM and visibility considering and not considering
 609 emission factors on 26 February 2014

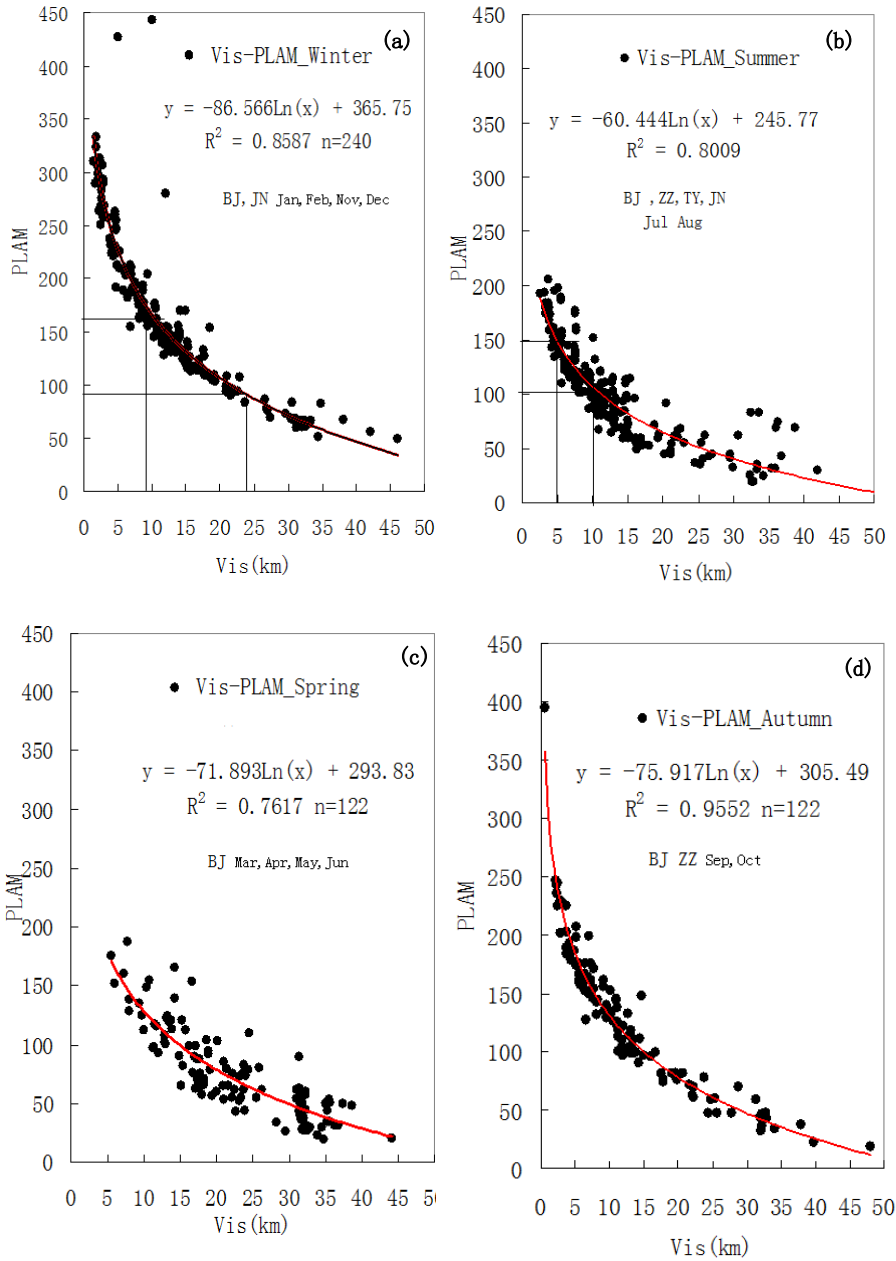


621 Figure 3 The cases for PLAM/h (a) and visibility (b) of the 14 April 2011 , PLAM/h (c)
 622 and visibility (d) of the 26 July 2008, PLAM/h (e) and visibility (f) of the 30 October
 623 2011 and PLAM/h (g) and visibility (h) on 7 January 2011



624
 625

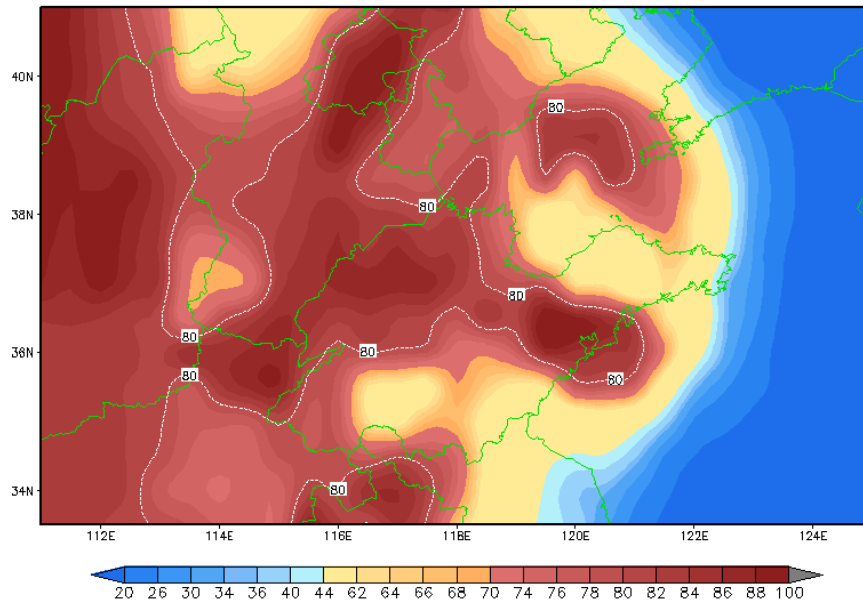
626 Figure 4 Correlation analysis of PLAM/h index and visibility in winter (a), summer (b),
 627 spring (c) and autumn (d)



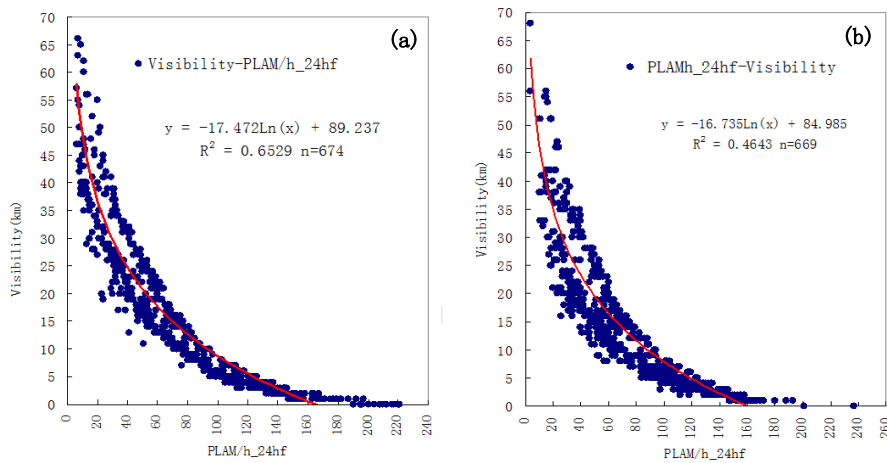
628

629

630 Figure 5 the regional correlation between PLAM/h index and visibility obtained by
 631 calculating the 1006 groups of observation samples collected from January 2009 to
 632 December 2012. The regional distribution of the correlation with significance level
 633 exceeding 0.001



634 Figure 6 the correlation analysis results of PLAM/h index 24 h forecasts and observed
 635 visibility respectively at 08:00(UTC+8) 20(a) and 08:00(UTC+8) 22(b) February

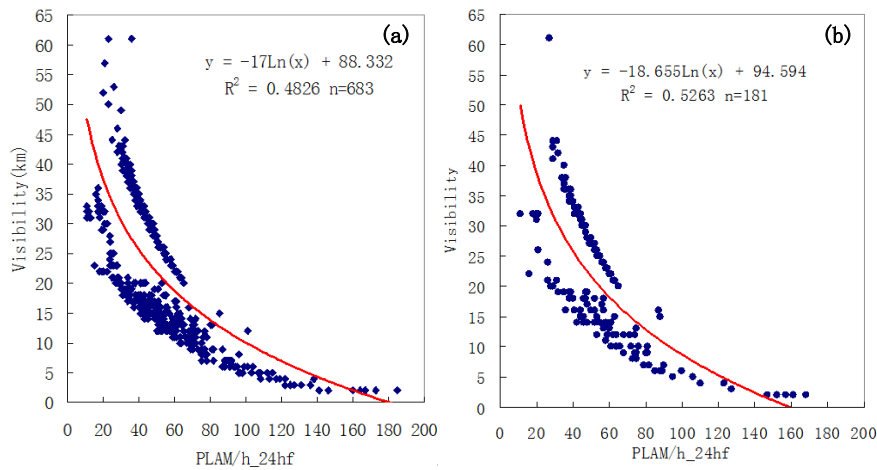


636 2014

637

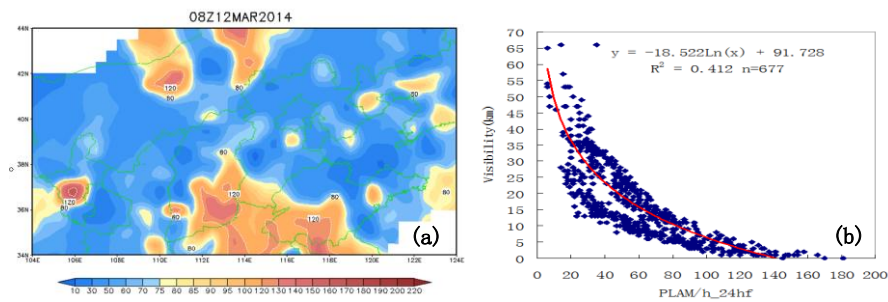
638

639 Figure 7 Correlation analysis of the regional PLAM/h index 24 h forecasts and
640 visibility during the whole period of pollution in North China respectively at
641 08:00(UTC+8) 20 (a)and 08:00(UTC+8) 22 July 2014(b)
642



643

644 Figure 8 distribution of PLAM/h in North China (a)and the correlation analysis of
645 PLAM/h index 24 h forecasts and observed visibility in North China for
646 8:00(UTC+8) March 12, 2014 (b)
647



656

657